Observed and Simulated Energy Cycles in the Frequency Domain

JIAN SHENG*

Program in Atmospheric and Oceanic Sciences, Princeton University, Princeton, New Jersey

YOSHIKAZU HAYASHI

Geophysical Fluid Dynamics Laboratory/NOAA, Princeton, New Jersey

(Manuscript received 22 August 1988, in final form 22 November 1989)

ABSTRACT

The analysis of spectral energetics in the frequency domain has been applied to several observed datasets and those simulated by a GFDL general circulation model. There exists good agreement on the directions of energy flows between the observed and the simulated atmospheres. The conversion from available potential energy to kinetic energy in the tropics and extratropics is the major source of eddy kinetic energy for all the low and high frequency bands discussed. The energy balance in the tropics has quite different characteristics from those in the extratropics. Instead of an up-scale decascade as in the case of the extratropics, kinetic energy is transferred in an opposite sense, namely from transients of longer time scales to those of shorter time scales.

Using a 5-year dataset from the ECMWF operational analysis, an energy cycle is obtained that is in general agreement with the one computed using the data of the FGGE year alone. The interannual variability of the spectral estimates is relatively small compared with the discrepancies caused by the variety of data origins.

1. Introduction

In a preceding paper (Sheng and Hayashi 1988, hereafter denoted SH), an energy analysis in the frequency domain was applied to the Level IIIb datasets from the First GARP (Global Atmospheric Research Program) Global Experiment (FGGE) processed at the Geophysical Fluid Dynamics Laboratory (GFDL) and the European Centre for Medium Range Weather Forecasts (ECMWF). The scheme used followed Hayashi (1980), which permitted a spectral view of atmospheric energetics as a function of frequency and diagnosed interactions among disturbances of different time scales. Among the results presented, it was demonstrated that the baroclinic conversion from available potential energy (APE) to kinetic energy (KE) played a major role in the energetics of maintaining both high frequency (periods shorter than 10 days) and low frequency (periods longer than 10 days but shorter than the annual cycle) motions. Another important observation found was that a substantial amount of KE was transferred by nonlinear interactions from the high frequency transients into the low frequency transients. On the other hand, APE flowed in the opposite direction, namely from the slow to fast transients. Therefore, in the frequency domain, there exists an up-scale decascade of KE and a down-scale cascade of APE. As shown in Fig. 1 (from SH), the energy balance of high frequency transients, averaged over the Northern Hemisphere, is very similar to the classic diagram given by Oort (1964); i.e.,

$$A(0) \Rightarrow A(n) \Rightarrow K(n),$$

where $A(n)$ and $K(n)$ are the APE and KE of the fast transients and $A(0)$ is the APE of the time mean. For the low frequency transients, although baroclinic conversion is the most important energy supply, the nonlinear exchange of KE results in some complications. The ECMWF analysis of the FGGE year indicates the amount of KE gained through nonlinear exchange is comparable to the baroclinic conversion at the low frequency range, while it is only of secondary importance for the GFDL analysis. On the other hand, the gain of APE due to nonlinear interactions is very small in the low frequency range. Equally important is that the effect of barotropic energy conversion, denoted by $\langle K(0) \cdot K(n) \rangle$ in the diagram, stabilizes disturbances of both high and low frequencies, although its magnitude is relatively small in comparison with the baroclinic conversion term $\langle A(n) \cdot K(n) \rangle$.

One of the goals of this paper is to discuss the variability of energy parameters as functions of latitude and height. In particular, the energy cycles will be es-

* Present affiliation: Department of Meteorology, McGill University, Montreal, Quebec, Canada.

Corresponding author address: Dr. Jian Sheng, Dept. of Meteorology, McGill University, 805 Sherbrooke Street, Montreal, Quebec, Canada H3A 2K6.

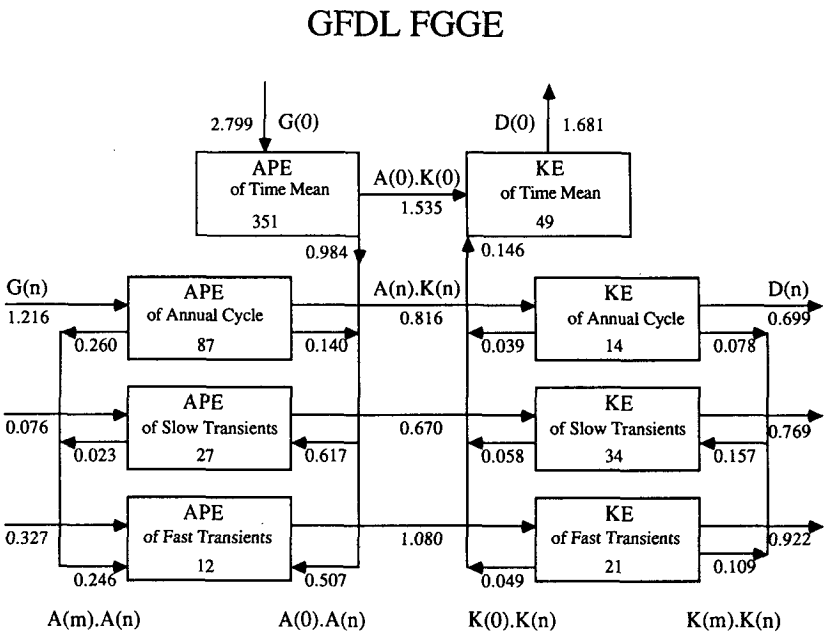

FIG. 1. Schematic depiction of the atmospheric energy cycle in the frequency domain estimated from the GFDL data of the FGGE year. Numbers in boxes denote the energy storage in 10^4 J m^{-2}, and fluxes of energy are in W m^{-2}. (From SH.)

timated separately for the middle latitudes and the tropics. The results discussed in SH, though hemispherically integrated, are essentially representative of the extratropics, since the intensity of transient activity is weaker in the tropics than in the middle latitudes. Studies of energetics (Kanamitsu et al. 1972, among others) indicate that energy balance in the tropics may be quite different from the extratropical regions. Although Plumb (1983) and Hayashi (1987) discussed the limitations of energetics in interpreting the dynamics of atmospheric motions, there is still enough interest to contrast the energetics of the tropics with that of the extratropics.

The analysis of frequency energetics has been applied to the atmosphere simulated by a GFDL general circulation model (GCM). The importance for the simulated atmosphere to agree energetically with that observed is apparent. Another subject of this investigation is the error in spectral estimates due to frequency aliasing. In the results of SH, observed once daily data were used for all calculations. Therefore, the Nyquist frequency corresponds to a period of 2 days and oscillations with periods shorter than 2 days are subject to aliasing. To examine the seriousness of the errors, a special experiment was designed in which the daily averaged vertical velocity was calculated. Energy conversion terms, estimated with the use of instantaneous and averaged vertical velocities, are compared to clarify this issue.

One pertinent concern in studies of the energetics of the global atmospheric circulation has always been the availability of meteorological observations in terms of spatial coverage as well as accuracy. Taken as a whole, the FGGE datasets represent the best global observations to date (especially in the tropics). In this study, however, a dataset of multiyear coverage is required in order to investigate the sensitivity of the spectral estimates to the choice of record length, and to evaluate the interannual variability of the energy cycle in the frequency domain. For this purpose the present calculations are extended to a 5-year dataset obtained from the ECMWF operational analysis.

In section 2, the scheme and the datasets for this study are briefly discussed. Section 3 discusses the latitude–pressure distributions of energy parameters and the contrast between the tropics and the extratropics. The energy cycle derived from the GFDL model is compared with the observations in section 4. The results of the multiyear data from the ECMWF are presented in section 5, with emphasis on the interannual variability and the sensitivity to the record length. The results are summarized in section 6. The impact of aliasing errors is discussed in the Appendix.

2. Energy equations and datasets

The spectral formulas used in this study have been described in Hayashi (1980), Sheng (1986) and SH. The scheme computes the nonlinear energy transfer spectra by use of the cross-spectral technique. Nonlinear product terms are calculated directly from the dependent variables without using the conventional

method of interactions of Fourier coefficients. This technique simplifies the calculations considerably and is applicable not only to frequency spectra but also to wavenumber or wavenumber-frequency spectra. An abbreviated description of the energy equations is provided in this section (for more details the reader is referred to SH). Based on Hayashi (1980), the equations of kinetic energy and available potential energy in the frequency domain are

$$0 = \langle K(m)\cdot K(n)\rangle + \langle K(0)\cdot K(n)\rangle + \langle A(n)\cdot K(n)\rangle + F(n) - D(n), \quad (1)$$

and

$$0 = \langle A(m)\cdot A(n)\rangle + \langle A(0)\cdot A(n)\rangle - \langle A(n)\cdot K(n)\rangle + G(n). \quad (2)$$

Terms in Eqs. (1) and (2) are interpreted as follows:

$\langle A(m)\cdot A(n)\rangle$	Transfer of available potential energy into frequency f_n by nonlinear interactions of transient disturbances.
$\langle A(0)\cdot A(n)\rangle$	Transfer of available potential energy into frequency f_n from the time mean.
$\langle A(n)\cdot K(n)\rangle$	Baroclinic conversion from available potential energy to kinetic energy at frequency f_n.
$\langle K(m)\cdot K(n)\rangle$	Transfer of kinetic energy into frequency f_n by nonlinear interactions of transient disturbances.
$\langle K(0)\cdot K(n)\rangle$	Transfer of kinetic energy into frequency f_n from the time mean.
$F(n)$	Convergence of energy flux associated with frequency f_n.
$G(n)$	Generation of available potential energy associated with frequency f_n.
$D(n)$	Dissipation of kinetic energy associated with frequency f_n.

One dataset used in this study is from the operational analysis of the ECMWF. It contains, on a 5-degree latitude–longitude mesh, wind components, geopotential height, and temperature once daily at the 100, 200, 300, 500, 700, 850, and 1000 mb pressure levels. The period is from 1200 UTC 1 January 1980 through 1200 UTC 31 December 1984. The vertical velocity is calculated kinematically from the continuity equation. Values of the calculated horizontal divergence are corrected by the method suggested by O'Brien (1970). It was indicated in Sheng (1986) that the vertical velocity computed from the ECMWF analysis was likely being underestimated even with the present kinematic method, as viewed from the strength of the Hadley cells.

A general circulation model developed at the GFDL, with rhomboidally truncated 30 wavenumbers (R30), is analyzed for comparison. The simulation covers one full year from 1 January to 31 December with data sampling taken once daily. To discuss aliasing errors the daily averaged vertical velocities are also saved for an R21 version of the model. The variables are vertically interpolated from the constant-σ coordinate onto pressure coordinate at 95, 205, 350, 515, 680, 830, and 940 mb levels. The data are then interpolated to grid systems roughly corresponding to 3.33×5.625 and 2.24×3.75 degree lat–long mesh, for the R21 and R30 models, respectively.

The two versions of the FGGE data from the GFDL and ECMWF analyses as described in SH are also used.

3. Latitude–pressure distributions of energy parameters

The distributions of the energy transformations as functions of latitude and pressure are given in Fig. 2 in the form of selected cross sections. The dataset is from the GFDL analysis of the FGGE year, which was used to calculate the energy cycle shown in Fig. 1. The parameters have been integrated over relatively wide spectral bands (2 to 10 days and 10 to 50 days) to represent the high and the low frequency transients, respectively. The integrand of $\langle K(0)\cdot K(n)\rangle$ is shown in Figs. 2a and 2b for the fast and slow transients, respectively. The most striking feature in Fig. 2a is a strong minimum centered slightly north of the annual mean position of the middle latitude westerly jet. A dipole pattern is seen in the upper level of the tropics and the net contribution from the low latitudes is small. Figure 2a is an interesting notion of the classical phenomenon of "negative eddy viscosity" (Starr 1968), evidenced by the negative value of $\langle K(0)\cdot K(n)\rangle$ around the jet stream. The distribution of the low frequency $\langle K(0)\cdot K(n)\rangle$ shows quite a different pattern (Fig. 2b). Unlike its high frequency counterpart the contribution from the lower latitudes is important for the hemispheric integration. On the other hand the integrand of $\langle K(0)\cdot K(n)\rangle$ changes sign at about 50°N and the net contribution from the middle latitudes is relatively small. The hemispheric average of this term turns out to be negative as discussed in SH, indicating that the time-mean flow is supported by the low frequency transients through the barotropic exchange of kinetic energy. This result is somewhat surprising. Wallace and Lau (1985), using 8 years of 300 mb wind data, calculated the barotropic conversion of kinetic energy from the time-mean flow to the transients at different frequency bands. Their results indicated that kinetic energy is transferred from the high frequency transients to the time-mean flow in agreement with the present estimates. For the low frequency band, however, the energy is transferred in the opposite direction; i.e., the flow is barotropically unstable to the low fre-

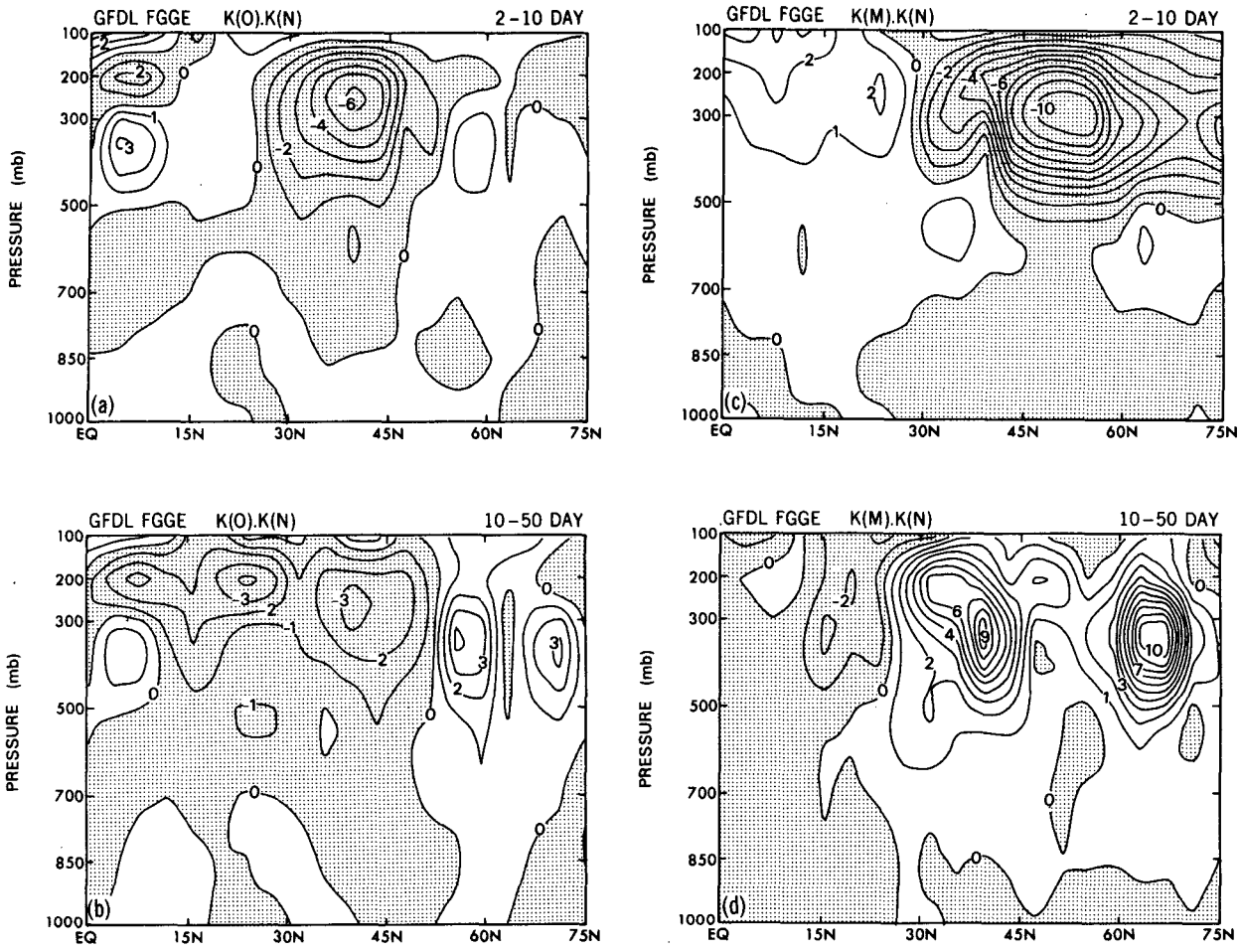

FIG. 2. Latitude-pressure cross sections of energy conversion terms for the high and low frequency bands. From the GFDL data of the FGGE year, in units of W kg^{-1}. Contour intervals: 2.0E-5. The negative regions are shaded (a) $\langle K(0)\cdot K(n)\rangle$ in the 2 to 10 day band, (b) $\langle K(0)\cdot K(n)\rangle$ in the 10 to 50 day band, (c) $\langle K(m)\cdot K(n)\rangle$ in the 2 to 10 day band, (d) $\langle K(m)\cdot K(n)\rangle$ in the 10 to 50 day band.

quency disturbances. Since their calculation covered the domain north of 20°N, the important negative contribution from the tropics (Fig. 2b) was not included.

Figures 2c and 2d show the nonlinear exchange of KE, $\langle K(m)\cdot K(n)\rangle$ for the high and the low frequency transients, respectively. For both frequency bands the contributions are mostly from the upper troposphere in the middle latitudes. Kinetic energy is lost from the high frequency band with a negative center at 50°N (Fig. 2c) and is gained in the low frequency band with two maxima located north and south of the negative center (Fig. 2d). Although the hemispheric averages are mainly due to the contributions from the extratropics, the lower latitudes consistently show sign reversals for both frequency bands. This is an indication that the nonlinear interaction of KE in the tropics takes the opposite direction of that in the extratropics. It is interesting to note that a similar observation was made in the wavenumber domain by Kanamitsu et al. (1972). Saltzman (1970) reviewed the energetics in the zonal wavenumber domain and concluded that both the short waves and planetary waves gain KE from the intermediate disturbances. In the tropics, however, zonal wavenumber 1 appears to be a major energy source, supplying KE to all other wavenumbers (Kanamitsu et al. 1972).

To address the difference in energy cycles between the tropics and the extratropics, estimates are made by taking integrations over these two parts of the atmosphere separately (see Figs. 3 and 4). The tropics are defined as the area between 20.625°S and 20.625°N, and the extratropics are the area north of 20.625°N. Since the present study is not concerned with a complete energy balance for these open domains, the energy flux term $F(n)$, the APE generation $G(n)$, and the KE dissipation $D(n)$ are not included in the analysis to simplify the discussion.

It is evident from comparison of Figs. 1 and 3 that the hemispheric average of the energy cycle essentially

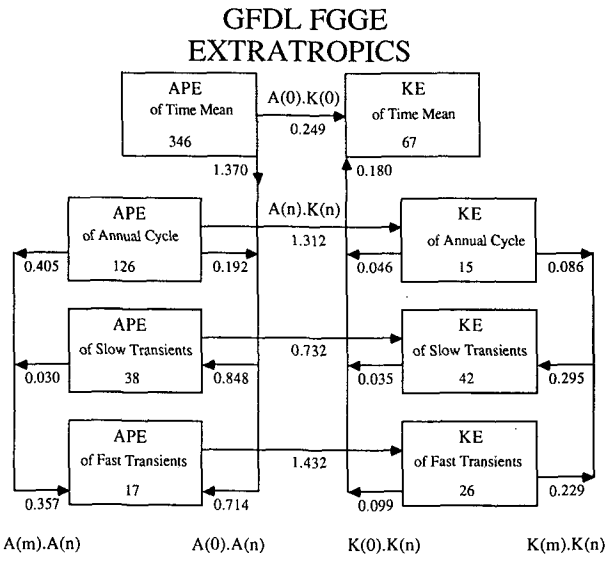

FIG. 3. As in Fig. 1, but for the extratropics. From the GFDL data of the FGGE year.

represents the energy balance in the extratropics. The hemispheric estimates generally take the same sign but have smaller magnitudes than those of the extratropical regions. One exception is the larger hemispheric conversion rate of $\langle A(0) \cdot K(0) \rangle$, which probably receives its major contribution from the Hadley cell in the tropics.

The energy cycle in the tropical region (Fig. 4) shows quite different features from the global estimate (Fig. 1). The tropics are characterized by very small values of APE, especially for the frequency of the annual cycle. The nonlinear interactions of APE are down to the noise level, whereas a sizable $\langle A(0) \cdot A(n) \rangle$ is observed. In contrast to the extratropics, the high frequency group appears to be barotropically unstable since kinetic energy is gained by the transients from the mean flow. As can be expected from the latitude-pressure cross sections (Figs. 2c and 2d) the direction of the nonlinear exchange of KE is reversed in the tropics and a cascade of KE from the longer to shorter time scales prevails. Interestingly, the magnitude of $\langle K(0) \cdot K(n) \rangle$ for the low frequency band (0.094 W m^{-2}) is nearly three times larger in the tropics than in the extratropics with the major contribution to the negative $\langle K(0) \cdot K(n) \rangle$ coming from the tropics. The dominant process to maintain the low frequency transients seems to be the baroclinic conversion term, $\langle A(n) \cdot K(n) \rangle$, as discussed in Krishnamurti et al. (1985).

The tropical intraseasonal oscillations have attracted much research interest after the FGGE data were made available. Numerous studies have focused on the structure characteristics and the mechanism responsible for generating and maintaining the oscillation (e.g., Murakami and Nakazawa 1985; Hayashi and Sumi 1986; Chen 1987). Although it is generally agreed that this low-frequency mode is a global-scale phenomenon (wavenumber 1 in zonal), it is frequently related to some regional convection regimes, such as convective activities in the equatorial western Pacific (Lau and Chan 1985). In theoretical and modeling studies, one usually invokes the concept of CISK (conditional instability of the second kind) to parameterize the diabatic heating generated by cumulus convection (Lau and Peng 1987; Chang and Lim 1989; Lau et al. 1989). From the energy cycle presented in Fig. 4 it is noted that, unlike in the extratropics, nonlinear interactions take away KE from the slow transients and the baroclinic conversion is the unique energy source for the low frequency KE. Also important is the fact that the low frequency APE is very weak. These features suggest that tropical convection plays a vital role in the maintenance of tropical intraseasonal oscillations. This is consistent with Knutson and Weickmann's (1987) results, which demonstrate that the vertical structure of the 30 to 60 day oscillations is baroclinic in the tropics, but equivalent barotropic poleward of about 20°N.

4. Energy cycles simulated by a GFDL general circulation model

The energy cycle simulated by the R30 version of a GFDL spectral model is shown in Fig. 5. The energy analysis has also been applied to the R21 version of the model and the results are similar (not shown). From a comparison with the FGGE year shown in Fig. 1, it is suggested that the difference between the two versions of the model appears smaller than that between the simulation and the observations. Thus the increase in resolution may not significantly improve the energy cycle in this case. A comparison of the energy conversion rates (shown in Fig. 5) with those corresponding to the GFDL FGGE analysis (Fig. 1) proves that the

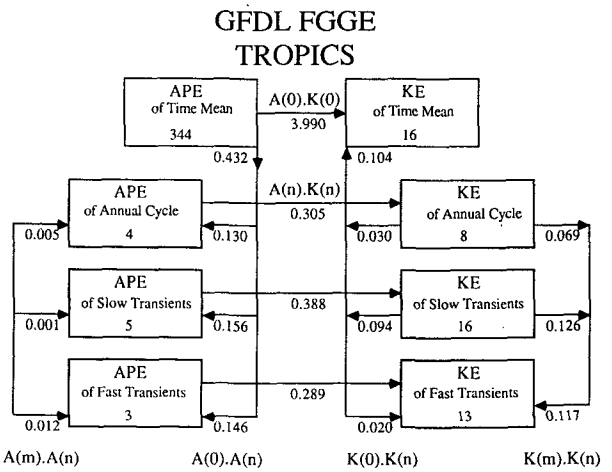

FIG. 4. As in Fig. 1, but for the tropics. From the GFDL data of the FGGE year.

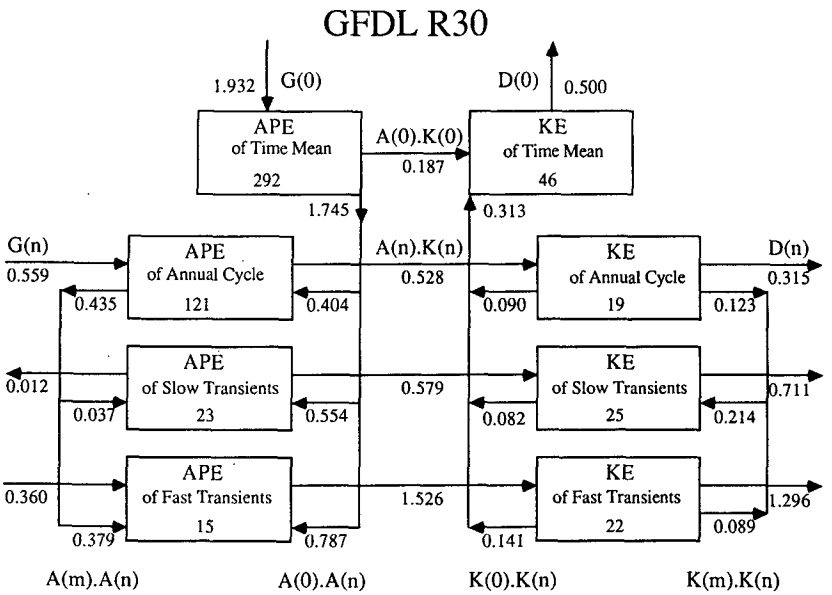

FIG. 5. As in Fig. 1, but for the R30 version of a GFDL model.

GCM is capable of simulating the energy cycle in the frequency domain, at least qualitatively, if not in quantitative detail. The following features should be noted:

(i) The energy level in the high frequency range is well simulated, in terms of the strength of the transient APE and KE. In the low frequency range, however, the level of model KE is lower in comparison with the observations. Furthermore, the simulated atmosphere undergoes a very strong annual cycle, as seen from the large values of APE and KE.

(ii) The simulated $\langle A(n) \cdot K(n) \rangle$ has positive conversions (from APE to KE) in all four groups of disturbances, in agreement with the observations. However, $\langle A(0) \cdot K(0) \rangle$, presumably with a major contribution from the Hadley cell, is much weaker than both versions of the FGGE analysis processed at GFDL and ECMWF, despite the fact that the ECMWF data has a conversion rate that is a factor of 3 smaller than the GFDL data (see SH). In section 5 it will be demonstrated that the interannual variability of $\langle A(0) \cdot K(0) \rangle$ in the 5-year data of the ECMWF analysis is rather small. Therefore, the discrepancy shown here indicates the sensitivity of this term to the data origins.

(iii) In agreement with observations, the model indicates a transfer of KE from the high frequency to the low frequency transients. On the other hand, the annual cycle in the model is actively involved in the nonlinear KE exchange, while its contribution appears less important in the FGGE year (Fig. 1). The role of the annual cycle is even more important in the nonlinear APE exchange since transients of the annual cycle supply APE to both fast and slow transients, in contrast to the observed energy loss by the slow transients. The active participation of oscillations associated with the annual cycle is consistent with the fact that the model simulates an annual cycle that is stronger than that observed. In accordance with the wavenumber-frequency energetics of the model, $\langle A(m) \cdot A(n) \rangle$ for the slow transients is small but positive (Hayashi and Golder 1983), although the FGGE data indicate a small negative value (Fig. 1).

The latitude-pressure sections of energy parameters are shown in Fig. 6. In Fig. 6a, the negative contribution of $\langle K(0) \cdot K(n) \rangle$ in the high frequency band is centered around the midlatitude jet stream and the pattern compares well with Fig. 2a. Unlike Fig. 2b, the strong contribution to $\langle K(0) \cdot K(n) \rangle$ of the slow transients is not from the tropics but from the position of the jet stream. The positive region centered around 60°N is much weaker and the strong midlatitude cancellation shown in Fig. 2b does not occur. One strong negative center in Fig. 2c and two strong positive centers in Fig. 2d are produced at the right positions, which contribute most to the global integrals of $\langle K(m) \cdot K(n) \rangle$ for the fast and slow transients (Fig. 6c and 6d). The reversal of $\langle K(m) \cdot K(n) \rangle$ in the tropics is strong for the high frequency band but weak for the low frequency band.

To isolate the tropics from the extratropics, calculated energy cycles are averaged in the region bounded by 21.5°S and 21.5°N, and the results of the R30 model are shown in Fig. 7. The overall agreement between Figs. 4 and 7 is reasonable. The small variances of APE and KE associated with the annual cycle are well simulated by the model. As observed during the FGGE year, the KE in the tropics is transferred nonlinearly in a direction opposite to its global average, namely the high frequency transients gain KE from the low frequency transients. The nonlinear exchange of APE is weak, as expected. The barotropic KE conversion is

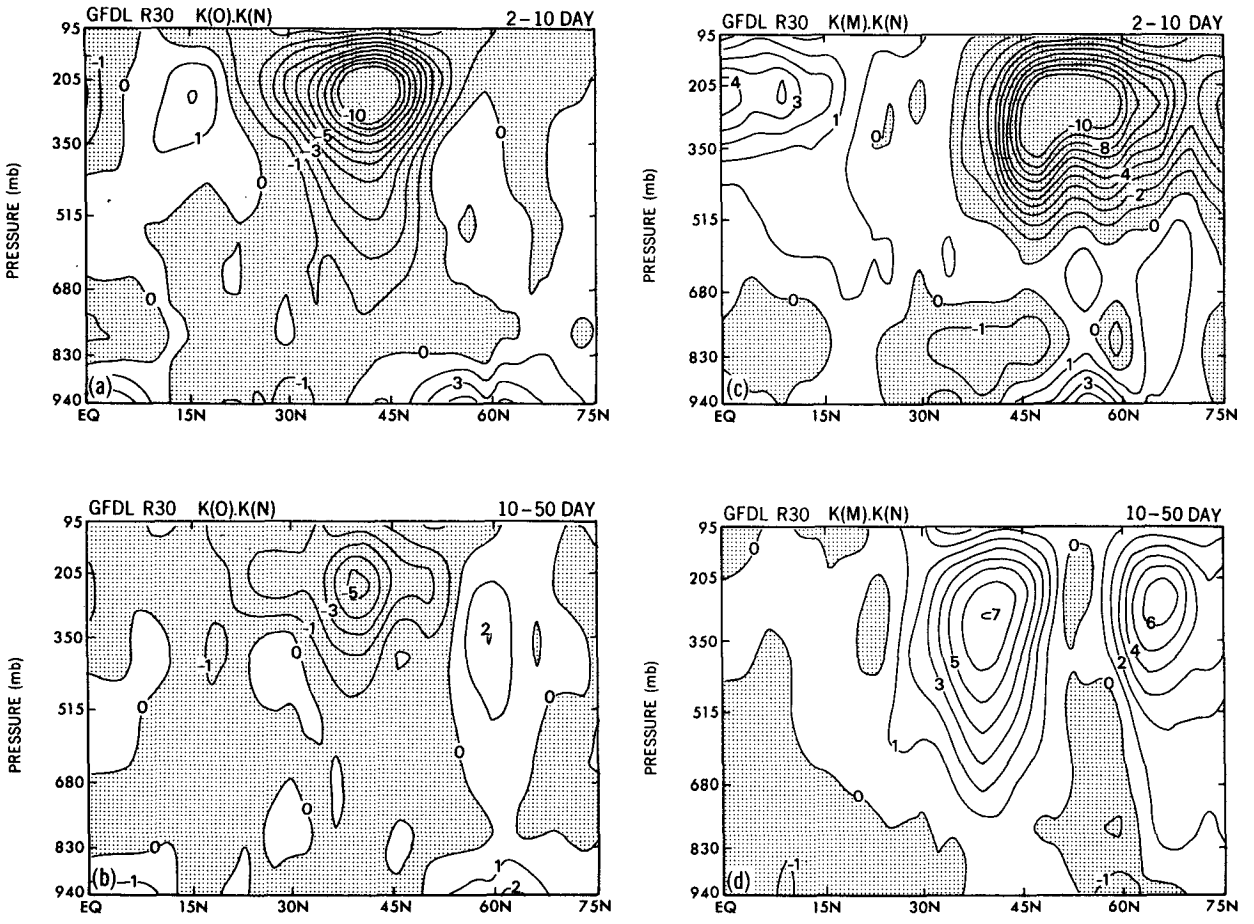

FIG. 6. As in Fig. 2, but for the R30 version of a GFDL model.

from the time-mean flow to the high frequency transients, which was also observed during the FGGE year.

Observationally, the global average of barotropic KE conversion from the time-mean flow to the low frequency transients is largely due to the contribution from the tropics (section 3). However, Fig. 7 indicates a smaller value of $\langle K(0) \cdot K(n) \rangle$; therefore, the global average of $\langle K(0) \cdot K(n) \rangle$ in the model is representative of the extratropics rather than the tropics. The marked difference in the barotropic KE conversion between the model and the FGGE analysis is evidently a reflection of the difference in relative strengths of the various regional features.

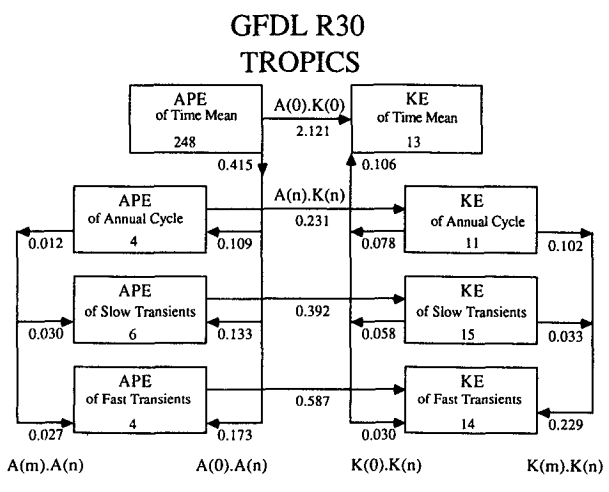

FIG. 7. As in Fig. 4, but for the R30 version of a GFDL model.

As can be concluded from the discussions in sections 3 and 4 the energy balance for the low frequency transients is complicated and the present results may be sensitive to possible errors such as frequency aliasing. This issue will be discussed in the Appendix.

5. The interannual variability of the energy cycle

The interannual variability of the energy cycle is studied using the 5-year dataset from the ECMWF. The spectral estimates of energy parameters are first calculated from the time series of a record length of 5 years (1827 days) and therefore the results are regarded as the mean estimates for the entire 5-year period. Next, the same calculation is repeated five times, each with

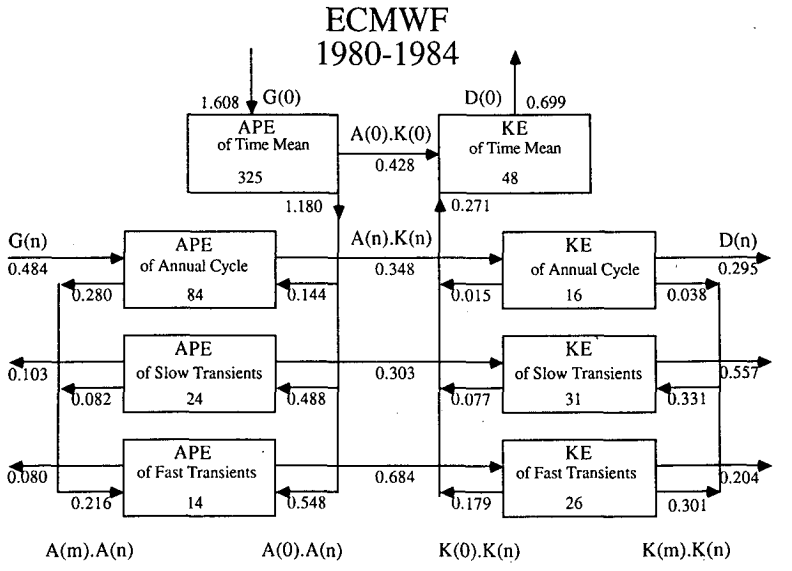

FIG. 8. As in Fig. 1, but for the ECMWF data of 1980–85.

one year of data. The estimates for individual years are then compared with those for the 5-year mean to evaluate the interannual variability.

As in SH, the energy and energy conversion terms are regrouped into four categories, those of time-mean, annual cycle, low frequency (periods longer than 10 days but shorter than the annual cycle) and high frequency (periods shorter than 10 days). The category of an interannual time scale is not included since the record length of 5 years may not be sufficient to provide statistically stable estimates for oscillations with periods longer than one year. The energy cycle is shown in Fig. 8, which should be compared with Fig. 10 in SH, representing the energy cycle for the ECMWF data of the FGGE year. The overall energetics agree very well with the previous study both qualitatively and quantitatively, although certain discrepancies in numerical estimates need more attention. One important difference is the energy balance in the low frequency region. It is seen that the gain from the nonlinear exchange of KE is increased from 0.299 to 0.331, whereas the baroclinic conversion term is almost unchanged. This increase results in the energy balance being slightly dominated by the nonlinear term $\langle K(m)\cdot K(n)\rangle$ instead of the baroclinic term $\langle A(n)\cdot K(n)\rangle$.

The interannual variability of the energy cycle is shown in Table 1. Each column in the table represents energy and energy conversion for one of the categories discussed above. The interannual variability is reasonably small such that the estimates for an individual year do not deviate much from the five year mean. The variations for the energy estimates are generally within 10 percent and the conversion terms keep the same sign for all five years, with one exception of $\langle A(n)\cdot K(n)\rangle$ at the annual cycle. In Table 1, the year-to-year difference of the energy cycle appears to be smaller than that between the GFDL and ECMWF data of the FGGE year. The stability of the spectral estimates, to some extent, provides the justification for using one year analysis (as in SH) to diagnose the energetics in the frequency domain, especially for the relatively high frequency bands.

A careful inspection of Table 1 leads to the conclusion that the estimates for lower frequencies tend to be less stable than those for higher frequencies, as can be seen in $\langle A(n)\cdot K(n)\rangle$ and $\langle A(m)\cdot A(n)\rangle$ of the low frequency group and in $\langle A(n)\cdot K(n)\rangle$, $\langle K(0)\cdot K(n)\rangle$, $\langle K(m)\cdot K(n)\rangle$ and $\langle A(0)\cdot A(n)\rangle$ of the annual cycle group. This is not surprising since they are of longer characteristic time scales and are not adequately sampled over the one year period to obtain stable statistics. On the other hand, part of the interannual variations should be attributed to the major system changes of data assimilation and analysis at ECMWF, as discussed by Trenberth and Olson (1988).

6. Conclusions

In the present study spectral energetics in the frequency domain have been applied to several observed and simulated datasets. The following conclusions have been reached:

(i) The tropics have distinctive features in maintaining the energy balance. The energy cascade of KE in the tropics shows a reversal from its direction in the extratropics, namely the high frequency transients gain KE from the low frequency transients. This feature is also observed in the GFDL model. It is of interest that

TABLE 1. Interannual variations of energy cycle (1980–84).

Year	Annual mean	Annual cycle	Low frequency	High frequency
		$K(n)$ (1.0E4 J m^{-2})		
1980	49	16	30	25
1981	47	16	32	27
1982	49	15	32	26
1983	52	19	31	26
1984	49	16	31	25
		$A(n)$ (1.0E4 J m^{-2})		
1980	316	81	22	13
1981	313	82	25	13
1982	338	83	25	14
1983	337	86	24	14
1984	340	92	29	13
		$A(n)\cdot K(n)$ (W m^{-2})		
1980	0.291	0.563	0.179	0.630
1981	0.390	0.537	0.289	0.649
1982	0.564	0.412	0.335	0.699
1983	0.457	−0.023	0.301	0.776
1984	0.421	0.298	0.367	0.701
		$K(0)\cdot K(n)$ (W m^{-2})		
1980	—	−0.015	−0.054	−0.181
1981	—	−0.024	−0.091	−0.187
1982	—	−0.006	−0.098	−0.196
1983	—	−0.013	−0.071	−0.168
1984	—	−0.027	−0.059	−0.185
		$K(m)\cdot K(n)$ (W m^{-2})		
1980	—	−0.038	0.307	−0.306
1981	—	−0.044	0.360	−0.284
1982	—	−0.039	0.335	−0.311
1983	—	−0.036	0.308	−0.317
1984	—	−0.012	0.352	−0.282
		$A(0)\cdot A(n)$ (W m^{-2})		
1980	—	0.193	0.449	0.583
1981	—	0.162	0.448	0.549
1982	—	0.073	0.487	0.557
1983	—	0.179	0.476	0.560
1984	—	0.158	0.524	0.516
		$A(m)\cdot A(n)$ (W m^{-2})		
1980	—	−0.281	−0.058	0.185
1981	—	−0.255	−0.092	0.204
1982	—	−0.274	−0.103	0.203
1983	—	−0.283	−0.105	0.234
1984	—	−0.325	−0.066	0.206

the major contribution to $\langle K(0)\cdot K(n)\rangle$ in the low frequency band comes from the low latitudes.

(ii) The GCM simulations at GFDL produce reasonable energy cycles in the frequency domain. The simulated energy cycles agree well on general directions of energy flow in the frequency domain with those observed in the real atmosphere. Reasonable energetics in the tropics are also produced.

(iii) The results of a 5-year calculation indicates that the interannual variability of the energy cycle in the frequency domain is relatively small, although the estimates of energetics for lower frequencies tend to be less stable than those for higher frequencies. Generally, the discrepancies among estimates from the different data sources are larger than the interannual variability. Therefore, the validity of the calculation in SH with the one year FGGE data is justified to some extent.

From the spectral energetics studied in SH and in the present paper, it is indicated, both by observations during the FGGE year and simulations at GFDL, that KE of the low frequency transients is maintained primarily through the conversion from APE. The APE of the low frequency transients is, in turn, maintained through the transfer from the time-mean flow. According to a numerical experiment (Hayashi and Golder 1987), on the other hand, nonlinear wave–wave transfer plays a more important role in the growth of ultralong waves than in their maintenance. Observationally, the low frequency transients are often associated with an equivalent barotropic structure with amplitude increasing with height (Blackmon et al. 1979). Theoretical studies on low frequency oscillations also suggest the importance of barotropic instability of the wintertime mean flow (Simmons et al. 1983). However, the present results call for a theoretical study to compare the roles of barotropic and baroclinic effects in generating and maintaining the low frequency transients. Schubert (1986) found that the net barotropic and baroclinic conversions were of comparable magnitude for periods greater than 10 days while the baroclinic conversion dominates for shorter periods.

Although the calculations with different datasets have provided energy cycles consistent with each other, we believe that until they are confirmed by the use of more accurate datasets the results must be considered tentative. The energy cycles presented are, if not qualitative, only semiquantitative. There is considerable room for future research in this area. The three-dimensional structure of the energy balance needs to be explored. In most earlier works (e.g., Oort and Peixoto 1974), general circulation statistics were presented in a zonally averaged format, which precludes any study of longitudinal differences. In more recent studies (e.g., Lau 1979), analyses are extended by processing data at all available pressure levels, which clearly illustrate that general circulation statistics exhibit strong longitudinal variations and geographic patterns. Due to the high order moments involved in the calculations of spectral energetics, integrations over wide frequency bands are essential for display of geographic patterns. It would also be of interest to separate the analysis into the winter and summer seasons. Although the fre-

quency of the annual cycle is lower than the fundamental frequency if a dataset covers the wintertime or summertime alone, the seasonal variation can be studied by contrasting energy cycles between the two seasons. The energy balance of interannual variations is also of interest. To obtain statistically stable estimates, observed or simulated datasets with a sufficient record length are necessary.

Acknowledgments. The authors are grateful to N.-C. Lau and D. G. Golder for their comments on the original manuscript. One of the authors (J.S.) is indebted to Prof. T. N. Krishnamurti for his encouragement and stimulating discussions on various aspects of this study. The figures were drafted by the Scientific Illustration Group at GFDL.

APPENDIX

An Assessment of Frequency Aliasing

The calculations presented thus far have all been based upon datasets with once daily sampling; therefore the Nyquist frequency in the spectral analyses corresponds to a frequency of a 2-day period. Transients with periods shorter than 2 days are aliased to those with periods longer than 2 days. An interesting example is the diurnal cycle due to the thermal forcing of the sun, which is the strongest signal beyond the Nyquist frequency (Vinnichenko 1970). Due to the sample interval of an exact day, the diurnal oscillation is aliased as part of the time-mean component. Since the main concern here is with the energy balance in the low frequency range, the aliasing of the strong diurnal cycle does not affect the discussion. It is important to note that aliasing errors cannot be completely eliminated by any smoothing technique or by reducing the sample intervals, as long as the atmospheric variables are sampled by discrete observations.

The impact of frequency aliasing is assessed by saving, once daily, the vertical velocity averaged over 24 hours as opposed to instantaneous values. Since the time step of integration for the R21 model is 6 minutes, it takes an unweighted average of 240 successive values. The reason the vertical velocity ω is chosen to estimate the error is simply that it is closely related to high frequency gravity waves and is more sensitive to frequency aliasing.

Figure 9 shows the spectra of the instantaneous and the averaged vertical velocity. The values indicated have been hemispherically mass averaged and the units are millibars per second squared. Unlike APE and KE the frequency distribution of the instantaneous ω is mostly concentrated at the high frequency end of the spectrum. The difference in power levels between the unsmoothed and the smoothed ω's significantly increases with frequency. The difference at the time-mean and the annual cycle is negligibly small—less than one percent. In the frequency band of 10 to 15 days the

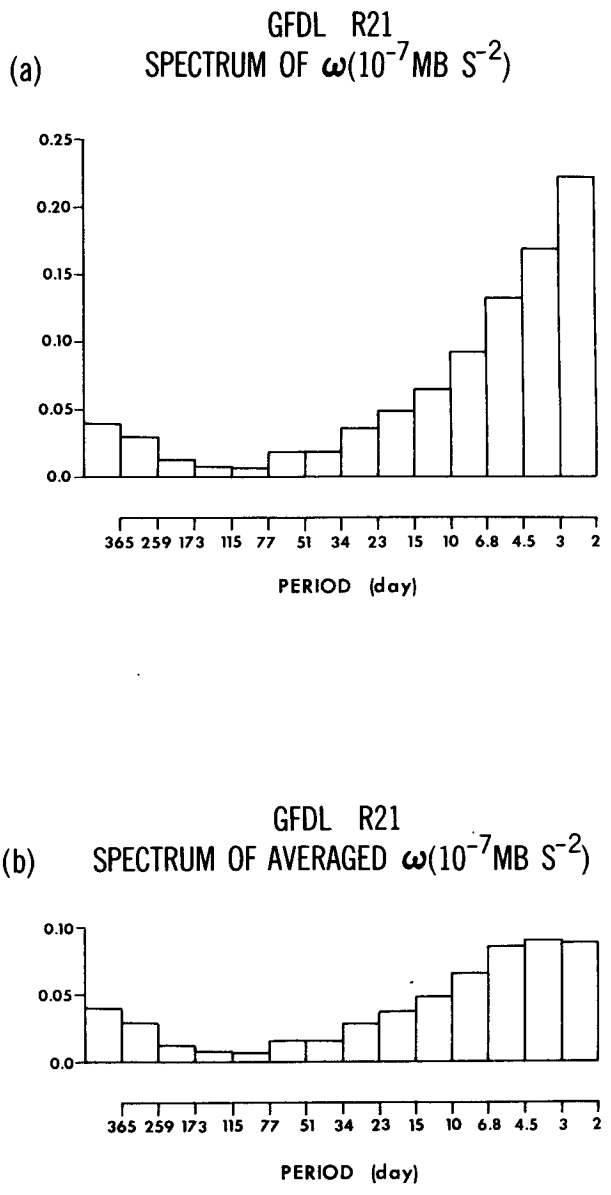

FIG. 9. Spectra of (a) the instantaneous, and (b) the averaged vertical velocities. The units are in millibars per second squared.

difference is still less than 25 percent. At the Nyquist frequency, however, the power in the smoothed ω drops down to 40 percent of the instantaneous ω. Bloomfield (1976) pointed out that the unweighted average modifies the spectral distribution such that the power at the Nyquist frequency is reduced to about 40 percent of the continuous data. Although the true spectrum is unknown in the present simulation, Fig. 9 suggests that the modification of the spectrum caused by using the instantaneous values is small.

The unweighted average in time has two effects on the shape of the spectrum. It not only removes from the spectrum aliasing errors but also modifies the spec-

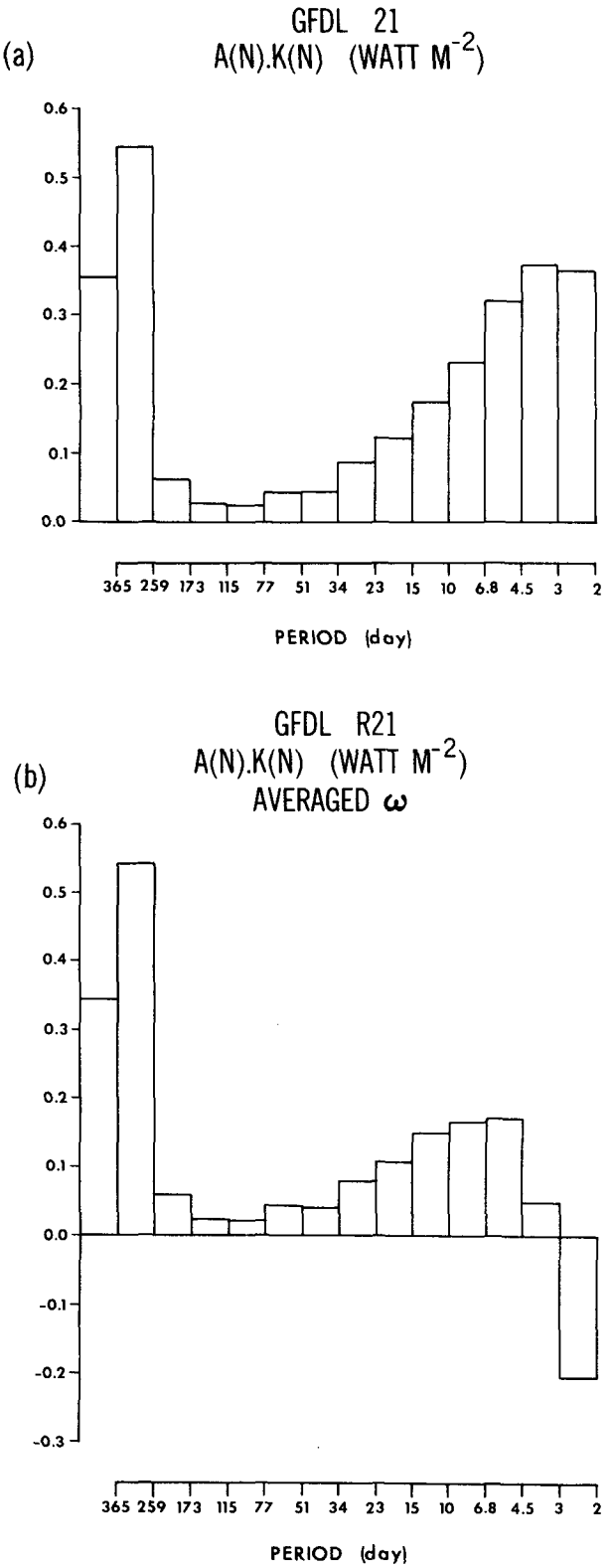

FIG. 10. Baroclinic conversion $\langle A(n) \cdot K(n) \rangle$ estimated with (a) the instantaneous, and (b) the averaged vertical velocities. The units are in W m^{-2}.

tral distribution. The baroclinic conversion terms $\langle A(n) \cdot K(n) \rangle$ calculated with the two sets of vertical velocities are shown in Fig. 10. It is seen that the difference between the two is relatively small in the low frequency region—less than 12 percent in the 10 to 15-day frequency band. The difference increases rapidly at high frequencies and the spectrum associated with the averaged ω becomes negative at the high frequency end. This negative value is probably due to the use of unaveraged temperature data.

In summary, the aliasing errors seem to have a relatively small impact on the low frequency part of $\langle A(n) \cdot K(n) \rangle$ but its impact may be more significant at the high frequency region. This issue can be better addressed if both vertical velocity and temperature are saved at a high resolution in time over a long period; however, GCM datasets of this kind are currently not available.

REFERENCES

Blackmon, M. L., R. A. Madden, J. M. Wallace and D. S. Gutzler, 1979: Geographical variations in the vertical structure of geopotential height fluctuations. *J. Atmos. Sci.*, **36**, 2450–2466.

Bloomfield, P., 1976: *Fourier Analysis of Time Series: An Introduction.* John Wiley & Sons, 259 pp.

Chang, C.-P., and H. Lim, 1988: Kelvin wave-CISK: A possible mechanism for the 30–50 day oscillations. *J. Atmos. Sci.*, **45**, 1709–1720.

Chen, T.-C., 1987: 30–50 day oscillation of 200-mb temperature and 850-mb height during the 1979 northern summer. *Mon. Wea. Rev.*, **115**, 1589–1605.

Hayashi, Y., 1980: Estimation of nonlinear energy transfer spectra by the cross-spectral method. *J. Atmos. Sci.*, **37**, 299–307.

——, 1987: A modification of the atmospheric energy cycle. *J. Atmos. Sci.*, **44**, 2006–2017.

——, and D. G. Golder, 1983: Transient planetary waves simulated by GFDL spectral general circulation models. Part II: Effects of nonlinear transfer, *J. Atmos. Sci.*, **40**, 951–957.

——, and ——, 1987: Effects of wave–wave and wave–mean flow interactions on the growth and maintenance of transient planetary waves in the presence of a mean thermal restoring force. *J. Atmos. Sci.*, **44**, 3392–3401.

Hayashi, Y. Y., and A. Sumi, 1986: The 30–40 day oscillations simulated in an "Aqua Planet" model. *J. Meteor. Soc. Japan*, **64**, 451–467.

Kanamitsu, M., T. N. Krishnamurti and C. Depradine, 1972: On scale interactions in the tropics during Northern Summer. *J. Atmos. Sci.*, **29**, 698–706.

Knutson, T. R., and K. M. Weickmann, 1987: 30–60 day atmospheric oscillations: Composite life cycles of convection and circulation anomalies. *Mon. Wea. Rev.*, **115**, 1407–1436.

Krishnamurti, T. N., P. K. Jayakumar, J. Sheng, N. Surgi and A. Kumar, 1985: Divergent circulations on the 30 to 50 days time scale. *J. Atmos. Sci.*, **42**, 364–375.

Lau, K.-M., and P. H. Chan, 1985: Aspects of the 40–50 day oscillation during the northern winter as inferred from outgoing long wave radiation. *Mon. Wea. Rev.*, **113**, 1889–1909.

——, and L. Peng, 1987: Origin of low-frequency (intraseasonal) oscillations in the tropical atmosphere. Part I: Basic theory, *J. Atmos. Sci.*, **44**, 950–972.

Lau, N.-C., 1979: The structure and energetics of transient disturbances in the Northern Hemisphere wintertime circulation. *J. Atmos. Sci.*, **36**, 982–995.

——, I. M. Held and D. J. Neelin, 1988: The Madden-Julian Oscillation in an idealized general circulation model. *J. Atmos. Sci.*, **45**, 3810–3832.

Murakami, T., and T. Nakazawa, 1985: Tropical 45 day oscillations during the 1979 Northern Hemisphere summer. *J. Atmos. Sci.*, **42,** 1107–1122.

O'Brien, J. J., 1970: Alternative solutions to the classical vertical velocity problem. *J. Appl. Meteor.*, **9,** 197–203.

Oort, A. H., 1964: On the estimates of the atmospheric energy cycle. *Mon Wea. Rev.*, **92,** 483–493.

——, and J. P. Peixoto, 1974: The annual cycle of the energetics of the atmosphere on a planetary scale. *J. Geophys. Res.*, **79,** 2705–2719.

Plumb, R. A., 1983: A new look at the energy cycle. *J. Atmos. Sci.*, **40,** 1669–1688.

Saltzman, B., 1970: Large-scale atmospheric energetics in the wave number domain. *Rev. Geophys. Space Phys.*, **8,** 289–302.

Schubert, S. D., 1986: The structure, energetics and evolution of the dominant frequency–dependent three dimensional atmospheric modes. *J. Atmos. Sci.*, **43,** 1210–1237.

Sheng, J., 1986: On the energetics of low frequency motions. Ph.D. dissertation, Florida State University, 171 pp.

——, and Y. Hayashi, 1990: Estimation of atmospheric energetics in the frequency domain during the FGGE year. *J. Atmos. Sci.*, **47,** 1255–1268.

Simmons, A. J., J. M. Wallace and G. W. Branstator, 1983: Barotropic wave propagation and instability, and atmospheric teleconnection patterns. *J. Atmos. Sci.*, **40,** 1363–1392.

Starr, V. P., 1968: *Physics of Negative Viscosity Phenomena.* McGraw-Hill, 256 pp.

Trenberth, K. E., and J. G. Olson, 1988: An evaluation and intercomparison of global analyses from the National Meteorological Center and the European Centre for Medium Range Weather Forecasts. *Bull. Amer. Meteor. Soc.*, **69,** 1047–1057.

Vinnichenko, N. K., 1970: The kinetic energy spectrum in the free atmosphere—1 second to 5 years. *Tellus,* **22,** 158–165.

Wallace, J. M., and N.-C. Lau, 1985: On the role of Barotropic energy conversion in the general circulation. *Adv. Geophys.*, **22A,** 33–74.